

Cite this: *Chem. Commun.*, 2012, **48**, 976–978

www.rsc.org/chemcomm

COMMUNICATION

Facile, mild and fast thermal-decomposition reduction of graphene oxide in air and its application in high-performance lithium batteries†

Zhong-li Wang, Dan Xu, Yun Huang, Zhong Wu, Li-min Wang and Xin-bo Zhang*

Received 7th October 2011, Accepted 23rd November 2011

DOI: 10.1039/c2cc16239c

We firstly propose a facile, mild and effective thermal-decomposition strategy to prepare high-quality graphene at a low temperature of 300 °C in only 5 min under an ambient atmosphere. Applying the advantage of this strategy that provides an oxidizing atmosphere, pure V₂O₅/graphene composite is successfully synthesized and exerts excellent lithium storage properties.

Graphene, a new class of two-dimensional (2D) nanomaterial consisting of a single layer of sp² network of carbon atoms, possesses extraordinary electrical, mechanical, and thermal properties.¹ These unique features offer great promise for many applications including nanoelectronics, supercapacitors, solar cells, sensors as well as batteries.² Up to now, graphene has been prepared by several approaches such as micromechanical exfoliation of graphite, chemical vapor deposition, epitaxial growth, and the reduction of graphene oxide (GO).³ However, the low productivity of the first three methods makes them unsuitable for large-scale applications and the reduction of GO becomes the most promising route for the bulk production of graphene.

The reduction of GO is usually fulfilled by chemical methods which relies heavily on different reductants such as hydrazine,⁴ dimethylhydrazine,⁵ hydroquinone,⁶ hydriodic acid with acetic acid,⁷ or sodium borohydride.⁸ Unfortunately, due to the toxicity of chemical reducing agents and multiple-steps, existing chemical approaches are inadequate for mass production of graphene. Recently, it is reported that GO can be reduced with thermal methods which are believed to be green methods without using any hazardous reductants. There have been two kinds of thermal methods reported: one is solvothermal reduction method and the other is solid heating reduction. However, the former method usually needs harsh solvents such as *N,N*-dimethylformamide or *N*-methyl-2-pyrrolidinone,⁹ high pressure,¹⁰ and/or long reacting time.¹¹ The latter method necessarily requires special atmosphere (ultra-high vacuum, Ar, H₂),¹² and/or rapid heating (>200 °C min⁻¹) up to 1050 °C under Ar gas or up to 800 °C under H₂ gas.¹³ It is still challenging to thermally reduce GO under mild conditions. What's even worse is that

the largely employed reducing ambience greatly hinders the preparation of graphene composite materials that necessarily require oxidizing atmosphere. Thereafter, it remains unexplored and highly desirable to develop a facile, mild and effective strategy to prepare graphene under oxidizing atmosphere to meet the challenge of far-reaching applications of graphene.

Herein, graphene is successfully prepared by a facile, low-cost and fast route by thermal decomposition of GO in air at low temperature of 300 °C (Fig. S1, ESI†) in only 5 min, wherein neither special atmosphere nor high temperature is employed, which endows this method suitable for large-scale applications. To the best of our knowledge, this is first time to successfully prepare graphene from solid GO under oxidizing atmosphere (21% O₂ in air), which opens up new opportunities in the development of graphene composite materials that necessarily require oxidizing atmosphere. Thanks to this advantage, pure vanadium pentoxide (V₂O₅) nanosheets/graphene composite, wherein the oxidizing atmosphere plays a critical role because V₂O₅ is apt to form a low valence compound, is successfully synthesized and exhibits excellent lithium storage properties including good cycle stability and high rate performance.

GO sheets are prepared following the literature procedure.¹⁴ Fig. S2a–c (ESI†) shows the scanning electron microscopy (SEM), transmission electron microscopy (TEM) and high-resolution transmission electron microscopy (HRTEM) images of ultrasonically exfoliated graphene oxide, which exhibits the typical wrinkle morphologies of GO. The thickness measured from the height profile of the atomic force microscopy (AFM) image (Fig. S3a, ESI†) is about 1.1 nm, indicating the formation of single-layer GO sheets. Thermal properties of GO under ambient atmosphere is first investigated as shown in Fig. 1a. From the thermogravimetry (TG) curve, it can be observed that there are three stages in the process of mass loss, including removal of adsorbed water at 100 °C, decomposition of oxygen-containing functional groups at 200 °C, and combustion of graphene at 550 °C. The corresponding differential thermal analysis (DTA) curve shows two strong exothermic peaks. We then focus on the electric property of the decomposition product of GO. Fig. 1b depicts the change of electrical conductivity of GO with different decomposition temperatures. Unexpectedly, it is found that the conductivity of GO after heating at 300 °C reaches to a remarkable value of 1068 S m⁻¹, more than five orders of magnitude higher than that of the

State Key Laboratory of Rare Earth Resource Utilization, Changchun Institute of Applied Chemistry, Chinese Academy of Sciences, Changchun, 130022, P. R. China. E-mail: xbzhang@ciac.jl.cn
† Electronic supplementary information (ESI) available: Experimental details and supplementary figures. See DOI: 10.1039/c2cc16239c

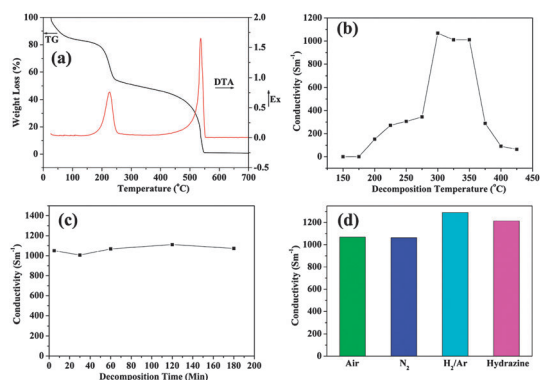


Fig. 1 (a) TG-DTA curve of GO, (b) the change of conductivity of GO decomposition products with different heating temperatures for 1 h in air, (c) the change of conductivity of GO decomposition products with different heating times at 300 °C in air, (d) conductivity comparison of the graphene prepared through four approaches (in air and N₂ at 300 °C, in 5% H₂/Ar at 550 °C, and in hydrazine solution at 95 °C).

pristine GO (0.006 S m⁻¹). Moreover, another interesting phenomenon is that the conductivity of GO decomposed at 300 °C for 5 min is similar to that for 3 h (Fig. 1c), indicating that the process of decomposition is very fast and the obtained graphene is stable in air at 300 °C even after a prolonged period. Fig. 1d compares the conductivity of graphene prepared through different approaches. Interestingly, all the conductivities are comparable, indicating that, like other chemical or thermal methods, our proposed thermal-decomposition reduction approach under air atmosphere is very effective toward deoxygenation of GO.

Fig. 2 and Fig. S2d (ESI†) display SEM, TEM and HRTEM images of graphene after thermal-decomposition reduction at 300 °C under ambient atmosphere. The single or few-layer graphene with lots of wrinkles is observed. Corrugation and scrolling are part of the intrinsic nature of graphene, due to the 2D membrane structure becoming thermodynamically stable *via* bending. From the edge of a large sheet, the thickness of graphene is measured to be around 1 nm by the height profile of the AFM image (Fig. S3b, ESI†), suggesting that the individual sheets are still preserved. After the thermal treatment, the sharp X-ray diffraction peak of GO (at $2\theta = 10.3^\circ$) disappeared, but a new broad diffraction peak (at $2\theta = 24^\circ$) appears (Fig. S4, ESI†), indicating the deep reduction of GO and the exfoliation of the layered graphene sheets.

The decomposition of oxygen-containing groups in GO is also confirmed by FT-IR spectroscopy. As shown in Fig. S5a (ESI†), the characteristic peaks of GO appear for O–H (3400 and 1410 cm⁻¹), C=O (1726 cm⁻¹), epoxy C–O (1228 cm⁻¹) and alkoxy C–O (1059 cm⁻¹). After the thermal treatment, the

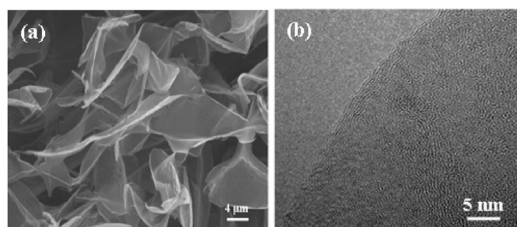


Fig. 2 SEM (a) and HRTEM (b) images of reduced GO at 300 °C for 1 h in air.

peaks for oxygen functional groups are reduced significantly, and the peaks for O–H, and alkoxy C–O are nearly entirely removed and the peak for C=O decreases dramatically. These observations confirm that most oxygen groups are successfully removed. The variation of the relative intensity of G (the E_{2g} mode of sp² carbon atoms) and D (the symmetry A_{1g} mode) bands in the Raman spectra of the GO during the reduction usually reveals the change of the electronic conjugation state. As depicted in Fig. S5b and Fig. S7 (ESI†), the intensity ratios (I_D/I_G) decrease from 1.14 of GO to 0.74 of graphene at 300 °C, which is lower than some chemical reduction reports, such as NaBH₄ (>1),⁸ hydrothermal reduction (0.90),^{15a} hydrazine hydrate (1.63),^{15b} implying the high efficiency of thermal-decomposition reduction. X-Ray photoelectron spectroscopy (XPS) measurements could provide the direct evidence of the reduction of GO during the thermal treatment. Fig. S6a and c (ESI†) show the C 1s XPS spectra of GO and thermal reduced graphene at 300 °C for 1 h, four different peaks centered at 284.7, 286.9, 288.2, and 289.0 eV, corresponding to C=C/C–C in aromatic rings, C–O (epoxy and alkoxy), C=O, and COOH groups, respectively, are detected. After thermal treatment, the intensities of all C 1s peaks of the carbons binding to oxygen, especially the peak of C–O (epoxy and alkoxy), decrease dramatically, in accordance with the FT-IR results. The C/O ratio changes from 2.3 to 5.7, indicating the efficient deoxygenation of GO and the formation of graphene. Although the ratio is lower than that (10.1) of reduced GO in H₂/Ar at 550 °C (Fig. S6e, ESI†), the degree of the thermal-decomposition reduction in air at 300 °C is similar to the typical chemical reduction process. Combining the changes of conductivity, I_D/I_G ratios, and C/O ratios with temperatures (Fig. 1b and Fig. S7 (ESI†)), it is found that all the data have the best values at 300 °C, indicating that the efficiency of thermal-decomposition reduction is greatly affected by the temperature, and the optimized temperature range is 300–350 °C according to the change of conductivity. Combining the above results with the latest report that GO decomposition releases O₂, CO and CO₂,¹⁶ it can be speculated that decomposition reactions of GO might contain one or more disproportionation reactions with the oxidation of functional groups and the reduction of the carbon framework.

V₂O₅ is a very-promising electrode material as it offers the attractive advantages of low-cost, abundant sources and better safety.¹⁷ Unfortunately, so far its practical application in rechargeable lithium ion batteries is still seriously hindered by the high rate performance and poor cycle stability.¹⁸ One of the most promising strategies to tackle this obstacle is to construct hybrid materials with fascinating graphene, however, wherein the purity of V₂O₅ is rather poor because V₂O₅ is apt to be reduced into a low valence compound. For instance, V₆O₁₃ impurity is formed even in an inert atmosphere, N₂, at 350 °C (Fig. S8, ESI†). On the contrary, by employing the uncovered feasibility of GO reduction in air, pure V₂O₅ nanosheets/graphene composite can be successfully synthesized from (NH₄)₂V₆O₁₆ nanosheets/graphene oxide by directly heating in air at 350 °C for 1 h (Fig. S9, ESI†). The content of graphene is ~20 wt% (Fig. S10, ESI†). Interestingly, the V₂O₅/graphene composite exerts excellent lithium storage properties. Fig. 3 illustrates the outstanding high-power and high-energy

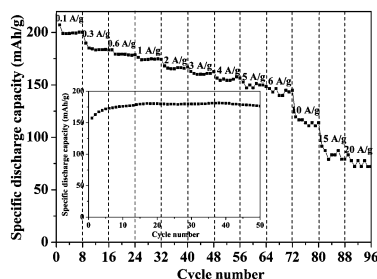


Fig. 3 Rate performance of the V_2O_5 nanosheets/graphene composite at different current densities from 0.1 A g^{-1} to 20 A g^{-1} , and the inset showing cycling performance at a current density of 0.3 A g^{-1} . All measurements are conducted with a voltage window of 2–4 V.

performance of the composite. At the current density of 6 A g^{-1} (20 C), the capacity can reach to 144 mAh g^{-1} , which is much higher than 90 mAh g^{-1} of V_2O_5 /carbon tube-in-tube composite at 5.88 A g^{-1} reported in the literature and other carbon-coated V_2O_5 ,¹⁹ and the corresponding power density is 16 kW kg^{-1} and energy density is 383 Wh kg^{-1} . From 199 mAh g^{-1} at 0.1 A g^{-1} (0.3 C) to 144 mAh g^{-1} at 6 A g^{-1} (20 C), the capacity retention remains as high as 72%, indicating the excellent rate capability. More importantly, even at the current of 20 A g^{-1} (67 C), there is still 73 mAh g^{-1} in the capacity, which delivers a very high power density of 48 kW kg^{-1} and energy density of 175 Wh kg^{-1} (Fig. S11a, ESI†). Typically, the power density of lithium ion battery's materials is in the range of 0.5 to 2 kW kg^{-1} .²⁰ The high-rate capability of the composite bridges the performance gap between batteries and supercapacitors. Moreover, the composite also exhibits good cycle stability and retains a high capacity of 178 mAh g^{-1} at the current density of 300 mA g^{-1} (1 C) (inset of Fig. 3). After 50 cycles, there is almost no decrease in capacity. From the discharge and charge curve (Fig. S11b, ESI†), the typical plateaus corresponding to the phase transitions of crystalline V_2O_5 are obviously observed. We can perhaps attribute these excellent lithium storage properties to the advantageous combination of graphene and V_2O_5 nanosheets, wherein the graphene acts as a good buffering matrix and provides a highly conductive network. The impedance spectroscopy (Fig. S11c, ESI†) shows that the resistivity of the cells is only 61Ω after 100 cycles. The above results further support the high quality of graphene after fast thermal-decomposition reduction in air.

In summary, we have demonstrated a facile and effective thermal-decomposition reduction method for scalable synthesis of high quality graphene from GO in air at a low temperature of $300 \text{ }^\circ\text{C}$ in only 5 min. This is the first reduction method that is carried out in oxidizing atmosphere. With the help of this intrinsic advantage, pure V_2O_5 nanosheets/graphene composite is successfully synthesized and exhibits excellent lithium storage properties. The proposed synthesis strategy may be easily extended to other graphene composites which can be used in broad fields including catalysis and sensors.

This work is financially supported by 100 Talents Programme of The Chinese Academy of Sciences, National Natural Science Foundation of China (Grant No. 21101147), and the Jilin

Province Science and Technology Development Program (Grant No. 20100102 and 20116008).

Notes and references

- 1 K. Geim and K. S. Novoselov, *Nat. Mater.*, 2007, **6**, 183.
- 2 (a) X. Li, X. Wang, L. Zhang, S. Lee and H. Dai, *Science*, 2008, **319**, 1229; (b) X. Wang, L. J. Zhi, N. Tsao, Z. Tomovic, J. L. Li and K. Mullen, *Angew. Chem., Int. Ed.*, 2008, **47**, 2990; (c) F. Schedin, A. K. Geim, S. V. Morozov, E. W. Hill, P. Blake, M. I. Katsnelson and K. S. Novoselov, *Nat. Mater.*, 2007, **6**, 652; (d) E. Yoo, J. Kim, E. Hosono, H. Zhou, T. Kudo and I. Honma, *Nano Lett.*, 2008, **8**, 2277.
- 3 (a) K. S. Novoselov, A. K. Geim, S. V. Morozov, D. Jiang, Y. Zhang, S. V. Dubonos, I. V. Grigorieva and A. A. Firsov, *Science*, 2004, **306**, 666; (b) K. S. Kim, Y. Zhao, H. Jang, S. Y. Lee, J. M. Kim, K. S. Kim, J. H. Ahn, P. Kim, J. Y. Choi and B. H. Hong, *Nature*, 2009, **457**, 706; (c) P. W. Sutter, J. I. Flege and E. A. Sutter, *Nat. Mater.*, 2008, **7**, 406; (d) S. Stankovich, D. A. Dikin, R. D. Piner, K. A. Kohlhaas, A. Kleinhammes, Y. Jia, Y. Wu, S. T. Nguyen and R. S. Ruoff, *Carbon*, 2007, **45**, 1558.
- 4 (a) V. H. Pham, T. V. Cuong, T. D. Nguyen-Phan, H. D. Pham, E. J. Kim, S. H. Hur, E. W. Shin, S. Kim and J. S. Chung, *Chem. Commun.*, 2010, **46**, 4375; (b) X. F. Zhou and Z. P. Liu, *Chem. Commun.*, 2010, **46**, 2611.
- 5 S. Stankovich, D. A. Dikin, G. H. B. Dommett, K. M. Kohlhaas, E. J. Zimney, E. A. Stach, R. D. Piner, S. T. Nguyen and R. S. Ruoff, *Nature*, 2006, **442**, 282.
- 6 G. X. Wang, J. Yang, J. Park, X. L. Gou, B. Wang, H. Liu and J. Yao, *J. Phys. Chem. C*, 2008, **112**, 8192.
- 7 (a) I. K. Moon, J. Lee and H. Lee, *Chem. Commun.*, 2011, **47**, 9681; (b) I. K. Moon, J. Lee, R. S. Ruoff and H. Lee, *Nat. Commun.*, 2010, **1**, 73.
- 8 H. J. Shin, K. K. Kim, A. Benayad, S. M. Yoon, H. K. Park, I. S. Jung, M. H. Jin, H. K. Jeong, J. M. Kim and J. Y. Choi, *Adv. Funct. Mater.*, 2009, **19**, 1987.
- 9 (a) H. L. Wang, J. T. Robinson, X. L. Li and H. J. Dai, *J. Am. Chem. Soc.*, 2009, **131**, 9910; (b) S. Dubin, S. Gilje, K. Wang, V. C. Tung, K. Cha, A. S. Hall, J. Farrar, R. Varshneya, Y. Yang and R. B. Kaner, *ACS Nano*, 2010, **4**, 3845; (c) W. F. Chen and L. F. Yan, *Nanoscale*, 2010, **2**, 559.
- 10 C. Nethravathi and M. Rajamathi, *Carbon*, 2008, **46**, 1994.
- 11 K. H. Liao, A. Mittal, S. Bose, C. Leighton, K. A. Mkhoyan and C. W. Macosko, *ACS Nano*, 2011, **5**, 1253.
- 12 (a) X. L. Li, H. L. Wang, J. T. Robinson, H. Sanchez, G. Diankov and H. J. Dai, *J. Am. Chem. Soc.*, 2009, **131**, 15939; (b) D. Yang, A. Velamakanni, G. Bozoklu, S. Park, M. Stoller, R. D. Piner, S. Stankovich, I. Jung, D. A. Field, C. A. Ventrice and R. S. Ruoff, *Carbon*, 2009, **47**, 145; (c) I. Jung, D. A. Dikin, R. D. Piner and R. S. Ruoff, *Nano Lett.*, 2008, **8**, 423; (d) X. Wang, L. J. Zhi and K. Mullen, *Nano Lett.*, 2008, **8**, 323.
- 13 M. J. McAllister, J. L. Li, D. H. Adamson, H. C. Schnlepp, A. A. Abdalam, J. Liu and I. A. Aksay, *Chem. Mater.*, 2007, **19**, 4396.
- 14 D. C. Marcano, D. V. Kosynkin, J. M. Berlin, A. Sinitskii, Z. Z. Sun, A. Slesarev, L. B. Alemany, W. Lu and J. M. Tour, *ACS Nano*, 2010, **4**, 4806.
- 15 (a) Y. Zhou, Q. L. Bao, L. A. L. Tang, Y. L. Zhong and K. P. Loh, *Chem. Mater.*, 2009, **21**, 2950; (b) J. Yan, Z. J. Fan, T. Wei, W. Z. Qian, M. Zhang and F. Wei, *Carbon*, 2010, **48**, 3825.
- 16 R. Larciprete, S. Fabris, T. Sun, P. Lacovig, A. Baraldi and S. Lizzit, *J. Am. Chem. Soc.*, 2011, **133**, 17315.
- 17 A. M. Cao, J. S. Hu, H. P. Liang and L. J. Wan, *Angew. Chem., Int. Ed.*, 2005, **44**, 4391.
- 18 (a) D. W. Liu and G. Z. Cao, *Energy Environ. Sci.*, 2010, **3**, 1218; (b) K. Kang, K. Song, H. Heo, S. Yoo, G. S. Kim, G. Lee, Y. M. Kang and M. H. Jo, *Chem. Sci.*, 2011, **2**, 1090.
- 19 (a) Y. S. Hu, X. Liu, J. O. Muller, R. Schlogl, J. Maier and D. S. Su, *Angew. Chem., Int. Ed.*, 2009, **48**, 210; (b) A. Odani, V. G. Pol, S. V. Pol, M. Koltypin, A. Gedanken and D. Aurbach, *Adv. Mater.*, 2006, **18**, 1431.
- 20 B. Kang and G. Ceder, *Nature*, 2009, **458**, 190.